5-1-1983

Ultrasonic Continuous Wave Spirometer

Todd A. Ell

ULTRASONIC CONTINUOUS WAVE
SPIROMETER

by

Todd A. Ell

Bachelor of Science, University of North Dakota, 1982

A Thesis

Submitted to the Graduate Faculty

of the

University of North Dakota

in partial fulfillment of the requirements

for the Degree of

Master of Science

Grand Forks, North Dakota

May

1983

This tnesis submitted by Todd A. Ell in partial fulfillment of the requirements for the Degree of Master of Science from the University of North Dakota is hereby approved by the Faculty Advisory Committee under whom the work has been done.

J. Hootman
(Chairperson)

Nagy N. Bengiamin

Edward Nelson

This Thesis meets the standards for appearance and conforms to the style and format requirements of the Graduate School of the Universiy of North Dakota, and is hereby approved.

A. William Johnson
Dean of the Graduate School

Permission

Title Ultrasonic Continuous Wave Spirometer

Department Electrical Engineering

Degree Master of Science

In presenting this thesis in partial fulfillment of the requirements for a graduate degree from the University of North Dakota, I agree that the Library of this University shall make it freely available for inspection. I further agree that permission for extensive copying for scholarly purposes may be granted by the professor who supervises my thesis work or, in his absence, by the Chairman of the Department or the Dean of the Graduate School. It is understood that any copying or publication or other use of this thesis or part thereof for financial gain shall not be allowed without my written permission. It is also understood that due recognition shall be given to me and to the University of North Dakota in any scholarly use which may be made of any material in my thesis.

Signature Todd Ell

Date April 28, 1983

TABLE OF CONTENTS

List of Illustrations

List of Tables

Acknowledgements

The author wishes to thank Professors Joe Hootman and Nagy Bengiamin for their assistance in the preparation of the ideas presented in this thesis.

ABSTRACT

There exists a problem of accurately performing spirographic measurements under physical stress situations. Existing systems, which use mechanical structures in the measurement process, have response times that are too slow, or are too bulky to be considered portable.

The proposed system solves these problems and has a number of attractive characteristics. The system uses relatively inexpensive solid state electronic components which implies a minimal of mechanical parts; portability; and a linear, fast response time.

The system presented in this thesis determines the velocity and temperature fluctuations of the human breath by measuring the difference and sum of the transit times for two continuous sound waves travelling in opposite directions along the air path. The information about the transit times is contained in the phase differences of the two sound waves across the path. A phase-locked loop is used to keep the differences across the path constant, irrespective of air - and sound - velocity variations. Therefore, the phase information is converted to frequency variations in the phase-locked loop.

CHAPTER 1

INTRODUCTION

The purpose of this thesis is to develop the design procedure for a portable, accurate spirometer - an instrument for measuring the breathing capacity of the human lungs - for use under varying physical stress.

Present systems, which involve some mechanical structure in the measurement process, have response times that are too slow, or are too bulky to be considered as portable.

The system designed solves these problems because of a number of attractive characteristics: relatively inexpensive solid state electronic components are used which implies a lack of moving parts and portability; and linear, fast response time and reliability.

The system determines the velocity and temperature fluctuations of the human breath by measuring the difference and sum transit times for continuous sound waves travelling in opposite directions along the air path. The information about the transit times is contained in the phase difference of the sound waves across the path.

A phase-locked loop (PLL) is used to keep the phase difference across the path constant, irrespective of air - and sound - velocity variations by changing the sound frequency. Therefore the phase information is converted to frequency variations.

Although the design is realizable with either an analogue or digital phase-locked loop, the digital phase-locked loop was choosen so that the frequency variation information is directly accessible in digital format. Thus, eliminating the need for analogue to digital converters. Digital information allows the use of a microprocessor for information processing/storage and, more importantly, digital control of the system.

CHAPTER 2

BASIC INSTRUMENT OPERATION

In this chapter we will show how the information contained in the phase shifts across the acoustic paths are converted into frequency variations of useful form.

The total system can be divided into two identical parts, each half determines the transit time of the sound waves traveling in one direction. Because there is no interaction between halves, this and all preceeding chapters will study the various responses of only one half of the system.

Figure 1 shows a simplified diagram of one-half of the measurement system. T is the transmitter, R and R' are the two receivers. The phase detector (PD), sequential loop filter (F) and digital controlled oscillator (DCO) form the phase-locked loop.

In general, a DPLL system consists of two main functional blocks, a phase comparator or detector, and a digital controlled oscillator. The DCO is set to operate at an angular frequency of ω_c in the absence of a digital control signal. When a control signal is present, then the instantaneous frequency deviation of the DCO is proportional to the control signal. The control signal comes from the PD whose output is proportional to the phase difference between two input signals, one of which is the output of the DCO.

To illustrate how a DPLL operates, assume that the loop is in lock at $t=0$ (i.e. the input freq./phase and output freq./phase of the DCO are equal), and that at $t=0+$ the input frequency changes by ω. At this time the phase detector output will give a positive signal to the DCO which in turn increases the frequency of the DCO. A new equilibrium point will be reached when the frequency of the DCO is equal to the frequency of the input signa . A filter is usually included in the control signal path to smooth the control signal.

The time it takes for a given phase plane of the transmitted sound wave to traverse the distances to the receivers are given by

$$T_1 = d_1/(c + v_a\cos\theta) \qquad (1)$$

and

$$T_2 = d_2/(c + v_a\cos\theta) \qquad (2)$$

where d_i is the separation between the transmitter and the receiver, c is the velocity of propagation of sound in still air, and $v_a\cos\theta$ is the velocity component of the air in the direction of the propagation of the sound.

The transmitted sound waves can be expressed as

$$T(t) = A\cos(\omega t + \phi')$$

where ω is the frequency in rad/sec and ϕ' is the initial phase output.

Knowing that each acoustic path introduces a time delay T_i; the received signals can be written as

$$R_i(t) = A\cos(\omega(t - T_i) + \phi').$$

Signal magnitude attenuation is neglected because the magnitude variations are eliminated from the received signals upon entering the phase detectors - provided the magnitude is sufficient to trigger them. Notice that this implies that the transmitted signal need not be sinusoidal but only periodic.

The input phase to the phase-locked loop is given by

$$\phi_i = K_{d3} \cdot \omega(T_2 - T_1) =$$

$$K_{d3} \cdot \omega(d_2 - d_1)/(c + v_a\cos\theta) \tag{3}$$

where K_{d3} is the gain constant of the phase detector.

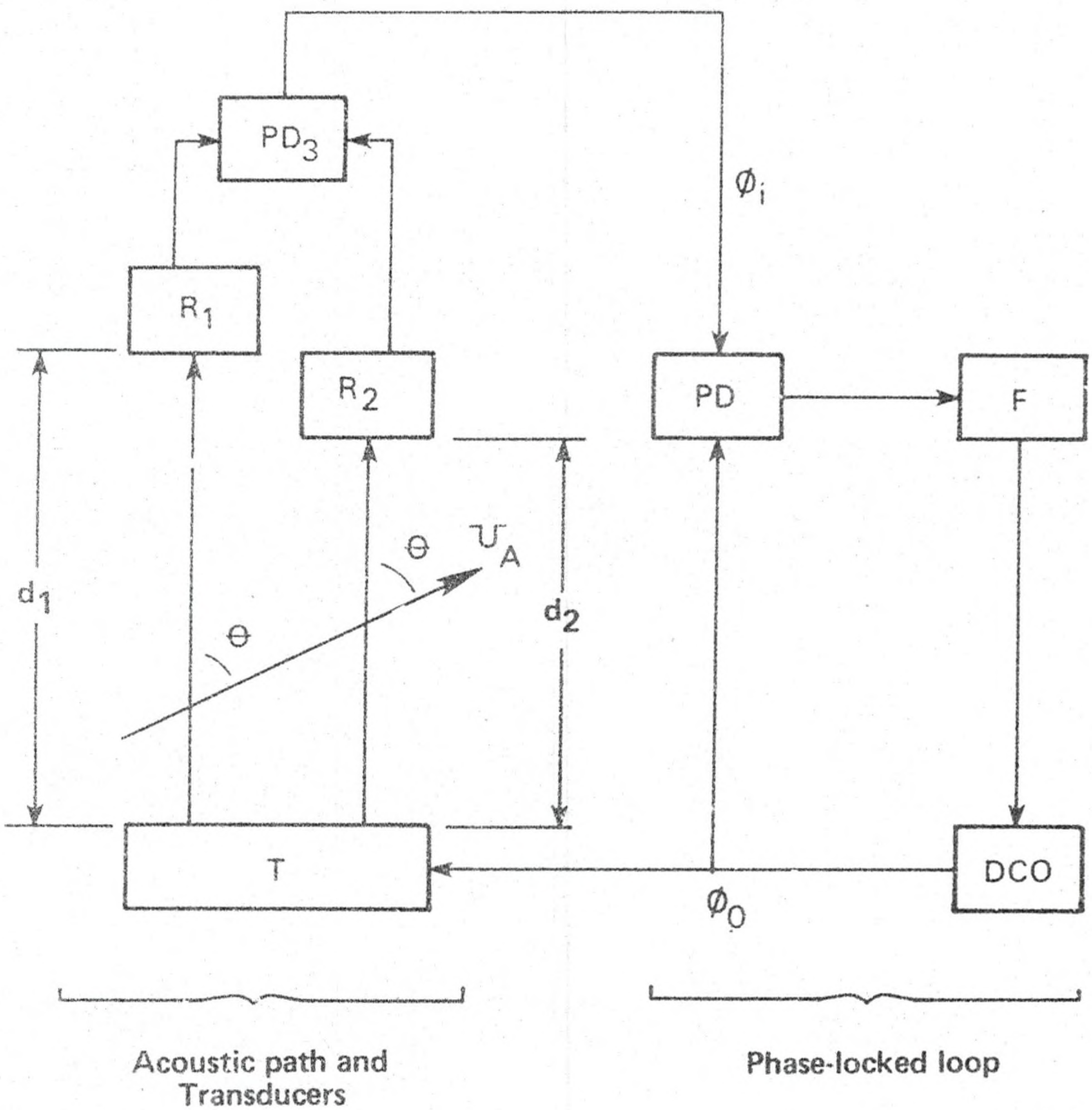

Figure 1. Schematic of one-half of system

The phase error ϕ_e, assuming the reference phase is zero (without loss of generality), is then given by

$$\phi_e = K_{d_3}\omega(d_2 - d_1)/(c + v_a\cos\theta). \tag{4}$$

The phase-locked loop phase detector output is zero for a given phase difference $\bar{\phi}$ (for this case $\bar{\phi} = (\frac{1}{2} \pm n)\pi$). If the differences between distances d_1 and d_2 are adjusted, under zero air velocity conditions, to give zero output from the phase detector, the output frequency will be the free running or center frequency ω_c. Under these conditions we obtain

$$\bar{\phi} = K_{d_3}\omega_c(d_2 - d_1)/c' \tag{5}$$

where c' is the velocity of propagation of sound at the time of adjustment.

Now, if $\phi_e \neq \bar{\phi}'$ the phase detector output will adjust the output frequency such that ϕ_e tends toward $\bar{\phi}'$. Assuming perfect phase-lock, (i.e. $\phi_e = \bar{\phi}'$) for all $T_2 - T_1$, and equating equations 4 and 5 we obtain

$$\frac{\omega - \omega_c}{\omega_c} = \frac{v_a\cos\theta}{c'} + \frac{c}{c'} - 1. \tag{6}$$

The same procedure can be used to derive the governing equation for the second half of the system.

$$\frac{\omega_1 - \omega_c}{\omega_c} = \frac{v_a\cos\theta}{c'} + \frac{c}{c'} - 1. \tag{7}$$

Summing and differencing (6) and (7), we obtain

$$\frac{\omega - \omega_{c1}}{\omega_{c1}} - \frac{\omega_1 - \omega_{c1}}{\omega_{c1}} = 2v_a \cos\theta/c' \tag{8}$$

$$\frac{\omega - \omega_{c2}}{\omega_{c2}} + \frac{\omega_1 - \omega_{c2}}{\omega_{c2}} = 2(c/c' - 1) \tag{9}$$

where ω_{c1} and ω_{c2} denote the two halves of the system.

The results of (6) and (7) show that the distances drop out of the equations and only relative frequency variations exist and need be measured.

Temperature variations are obtained from equation 9 using equation 10, given in [1] as

$$c = 331.5 + .607\, T_0 \ \text{m/sec} \tag{10}$$

where T_0 is the temperature in degrees centigrade.

A closer inspection of the basic system shown in figure 1 reveals that the system would operate in the same way if PD_3 were removed and only one acoustic path was incorporated into the system. This is true, and this method is exactly how an anemometer was built as given in [2].

The major reasons for not using the Single Path Anemometer method is to reduce cost and size. The derivations given earlier in this chapter assume that the transducers and receivers introduce no time delay. This is never the case, and the added delay introduces an error in the desired response of the system.

There are two methods of reducing this error. One method is to use expensive condenser microphones as transducers with very small delays. This is what was done in [3], at a very high cost (75% of the total system cost). The second method, which is used in this system, is to use relatively inexpensive matched Piezoceramic air transducers, which have a larger delay, and to reduce the effect of this delay by introducing a second acoustic path as a reference, within the PLL feedback path. Exactly how this is done is considered in chapters 4 and 5.

Notice that the assumption of a perfect phase-lock is made in the derivation of equations 8 and 9. This assumption is guaranteed by using a second order phase-locked loop which is perfect phase-locked as long as the frequency variations stay within the lock range of the PLL. This requirement introduces the possibility that the system may not be stable. Chapter 5 will deal with the stability of the proposed system.

CHAPTER 3

SYSTEM DESCRIPTION AND MODELING

In this chapter is a detailed description of the system and how each section is modeled. Figures 2 and 3 show the complete system schematic and a detailed schematic of the digital phase-locked loop, respectively.

Digital Phase-locked Loop Model

The model used for the digital phase-locked loop (DPLL) was taken directly from [4]. Although the DPLL and analogue phase-locked loop perform the phase-locking function by entirely different methods, linear control systems models for the loops are analogus, enabling the system to be constructed in either the digital or analogue world. This model is shown in figure 4. The parameters shown in figure 4 are defined in appendix E.

Acoustic Path Model

It is known that the acoustic paths introduce a time delay between the outputs and inputs of the transducers. Therefore, the input frequency and initial phase to the receivers can be written as

$$f_i(t) = f_0(t - T_i) \tag{11}$$

and

$$\phi_i'(t) = -f_0(t - T_i) \cdot T_i . \tag{12}$$

Because the PLL model operator is the total phase angle, as it differs from the rate caused by the loop center frequency f_c, these equations need to be modified for incorporation into the system model as follows.

The input phase ϕ_i, due to changes in frequency input and initial phase angle is for each path

$$\phi_i = \int_o^t (f_i - f_c)dt + \phi_i' \tag{13}$$

and the output frequency due to changes in rate of output phase ϕ_o, again, for each path is

$$f_o = f_c + d\phi_o/dt. \tag{14}$$

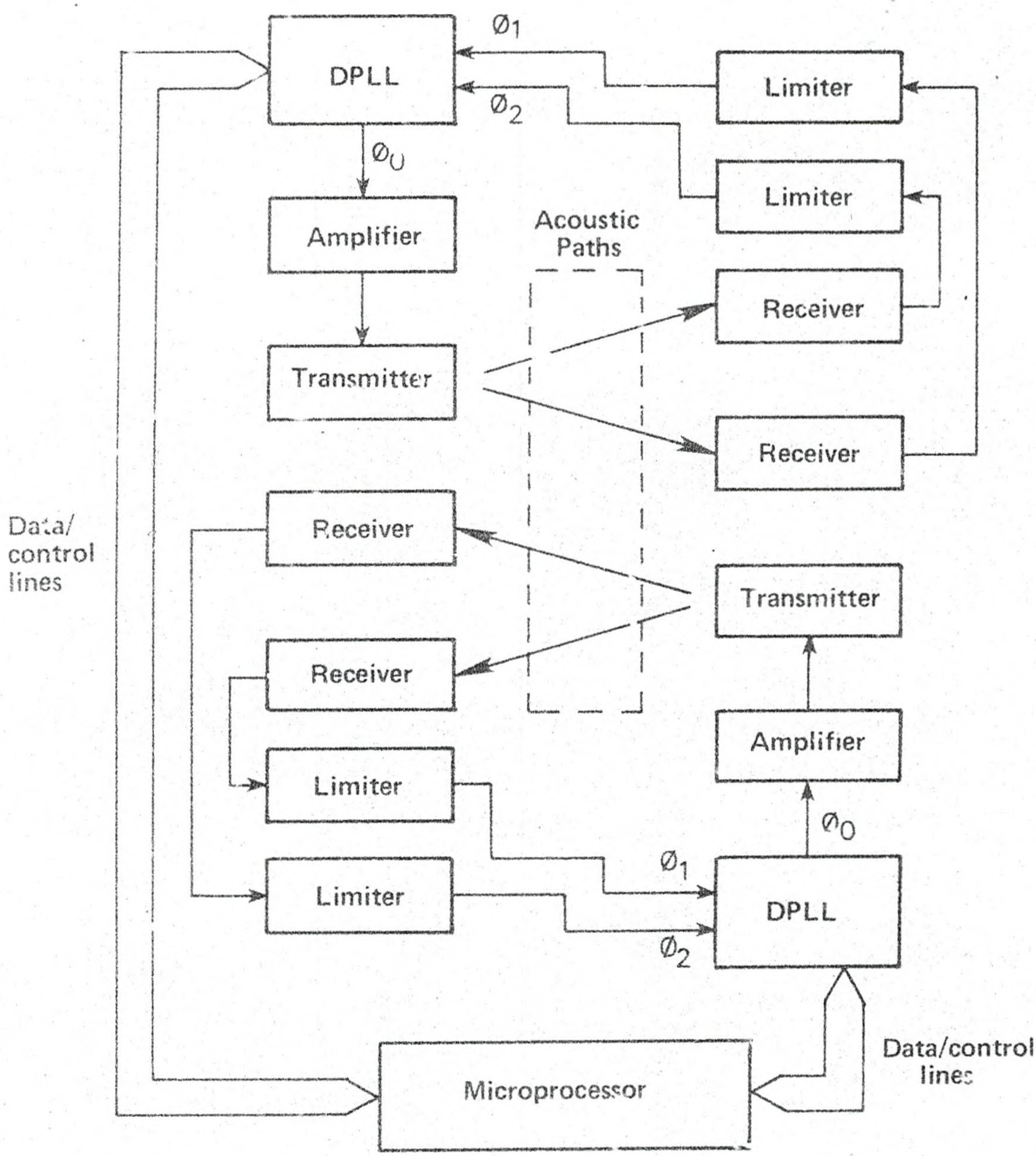

Figure 2. Complete system schematic.

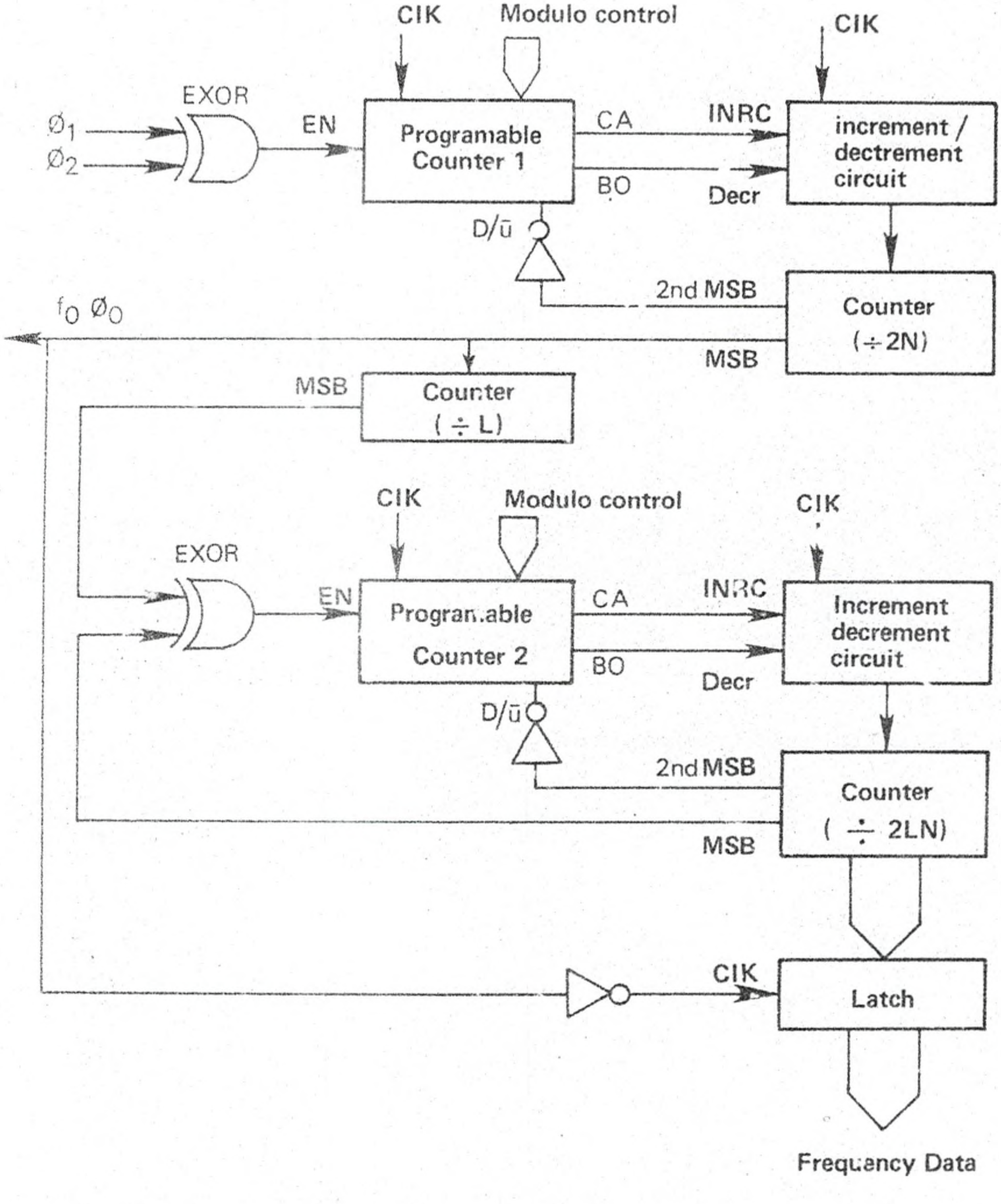

Figure 3. Schematic of Digital Phase - locked Loop.

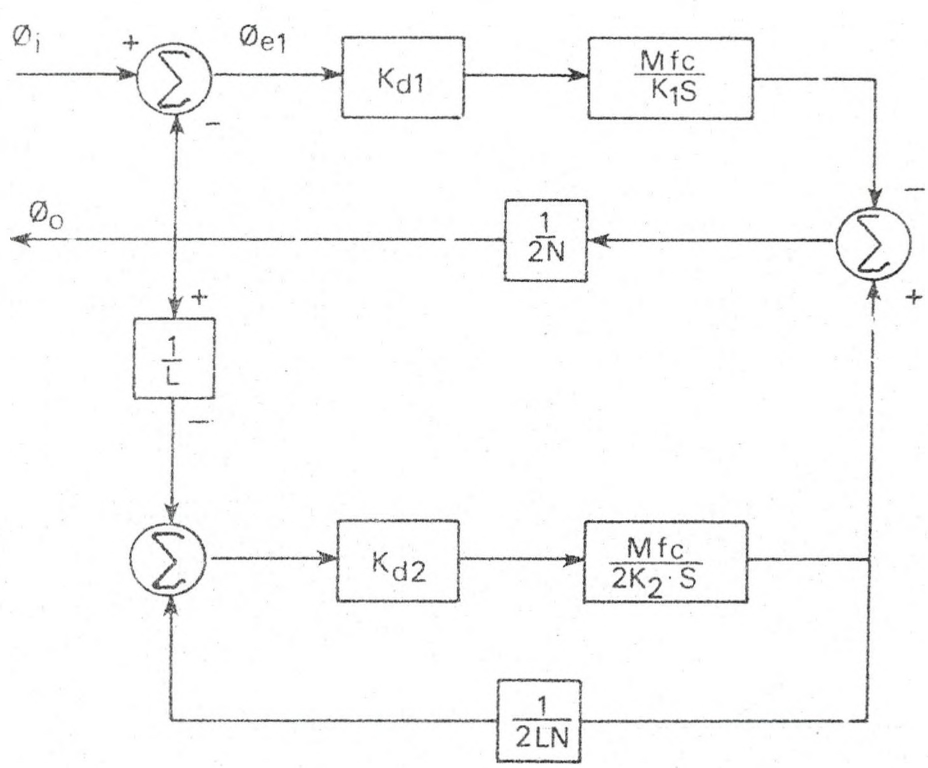

Figure 4. Linear controls systems model for second order Digital Phase-locked loop.

Combining equations 10, 11, 13 into 12 we obtain for

$$\phi_i = \int_0^t \{f_c(t-T_i)+d\phi_o(t-T_i)/dt - f_c(t)\}dt - \{f_c(t-T_i)+d\phi_o(t-T_i)/dt\}T_i$$

where i represents the path taken. Taking the Laplace transform of ϕ_i, assuming $f_c(t-T_i) = 0$ for $T_i > t$, results in

$$\phi_i(s) = \phi_o(s)(1 - sT_i)\cdot\exp(-sT_i) - f_c(s)\{(sT_i-1)\cdot\exp(-sT_i)+1\}/s. \quad (15)$$

Transducer - filter model

If the gain transfer function of the transducers and any filter inserted into the feed paths of the phase detectors to reduce noise is expressed in factored form as

$$T(s) = \prod_{i=1}^{n}(b_{1i}s^2 + b_{2i}s + b_{3i})/(b_{4i}s^2 + b_{5i}s + b_{6i}). \quad (16)$$

then the delay, using the definition given in [5], as

$$T_k = d(-\phi(\omega))/d\omega$$

can be written as

$$T_k(\omega) = \sum_{i=1}^{n}\{(-b_{2i}(b_{3i} + b_{1i}\omega^2)/((b_{3i} - (b_{1i}\omega)^2)^2 + (b_{2i}\omega)^2))$$
$$+(-b_{5i}(b_{6i} + b_{4i}\omega^2)/((b_{6i} - (b_{4i}\omega)^2)^2 + (b_{5i})^2))\} \quad (17)$$

If the changes in the output frequency ω_o from the center frequency ω_c are very small T_k can be approximated as a constant whos value is given by equation 17 with being replaced by ω_c. Therefore, the model for the transducers and filters will be simply a constant delay represented as $\exp(-T_K s)$.

The ideal transmitting response of a piezoceramic trasducer is defined by $T_T(s)$ in [6] as

$$T_T(s) = Ks^2/\{s^2 + (\omega_{nT}s/Q_T) + \omega_{nT}^2\}$$

The ideal receiving response of a piezoceramic transducer $T_R(s)$ is given by [7] as

$$T_R(s) = K/\{s^2 + (\omega_{nR}s/Q_R) + \omega_{nR}^2\}$$

where, in the previous equations, ω_n is the resonance frequency and Q is the quality of the transducers.

If the crystals are operated at their resonance frequency the corresponding delay constant is

$$T_K = 2(Q_T/\omega_{nT} + Q_R/\omega_{nR}).$$

Because the crystals have gain characteristics of a sharp bandpass filter, as shown in figure 5, further filtering is unnecessary.

Figure 6 shows the complete signal flow graph, for one-half of the system.

The relationship of the DPLL to the analog PLL and why the digital was choosen over the analoge can be explained by referring to figure 3. We see that if a divide-by-2LN counter with parallel outputs is incorporated into the phase-locked loop, the frequency offset information can be latched into a bank of registers by f_0 this eliminates the need for converting the output frequency into digital form for processing by a microprocessor, thus reducing the components needed for conversion into a bank of latches. With this technique a higher degree of accuracy may be attained by adding more stages to the divide-by-2LN counter and latch.

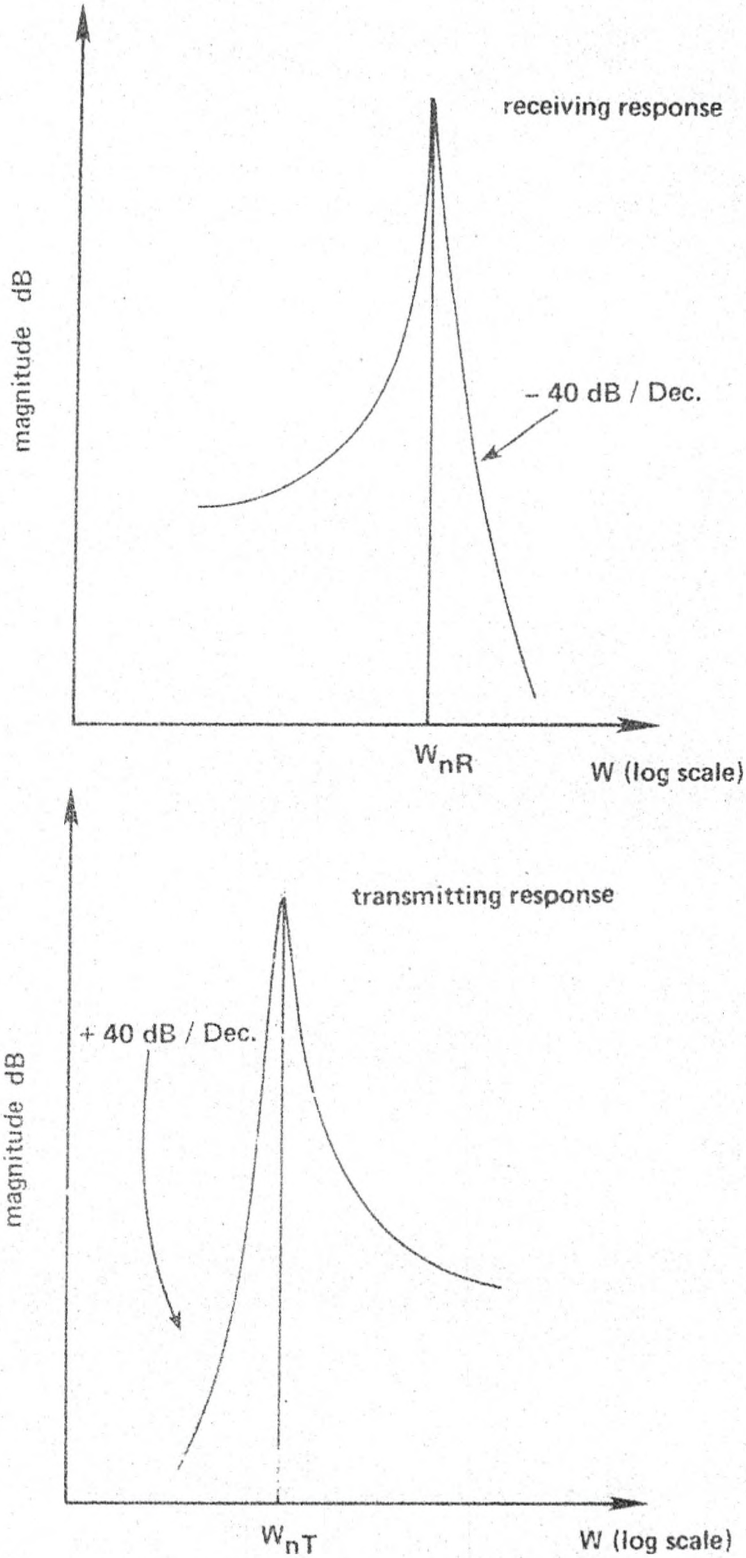

Figure 5. Ideal transmitting and receiving response for a piezoelectric transducer.

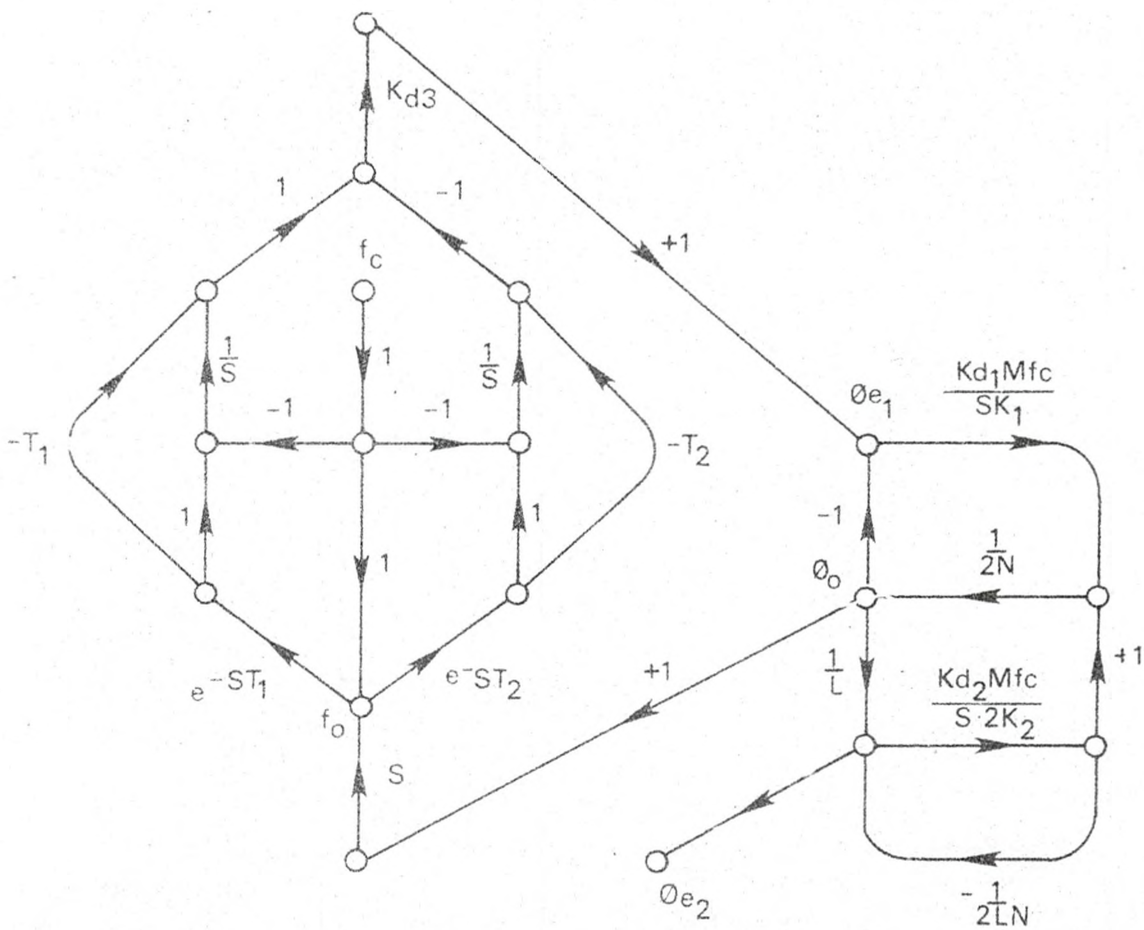

Figure 6. One-half the system in signal flow graph representation.

CHAPTER 4

STEADY-STATE RESPONSE

In this chapter, we will show how equations 8 and 9 are realized by the system under steady-state conditions (i.e. $\phi_{e1} = 0$, $v_a \neq 0$). We will first neglect transducer-filter delay and later address this problem in more detail. Under steady-state conditions ϕ_{e2} is given as [8]

$$\phi_{e2} = (4K_2N)(f_0 - f_c)/K_{d2}Mf_c.$$

Inserting equation 6 we obtain

$$\phi_{e2} = (4K_2N)\{(v_a\cos\theta)/c' + c/c' - 1\}/K_{d2}M$$

and from the other half of the system

$$\phi_{e2B} = (4K_2N)\{(-v_a\cos\theta)/c' + c/c' - 1\}/K_{d2}M.$$

The center frequencies must be different for each acoustic signal so that the signals do not interfere. The summing and differencing of the above equations yield

$$\phi_{e2} - \phi_{e2B} = (8K_2N)(v_a\cos\theta/c')/K_{d2}Mc' \tag{18}$$

and

$$\phi_{e2} + \phi_{e2B} = (8K_2N)(c/c' - 1)/K_{d2}M. \tag{19}$$

These equations assume perfect phase-lock. The second-order DPLL will track its incoming signal with zero phase error within its lock range.

The second-order DPLL lock range is given in [8] as

$$\Delta f_{max}/f_c = (f_{0_{max}} - f_c)/f_c = M/8K_2 N(1 + 1/2K_2)\ \text{Hz}. \qquad (20)$$

To determine proper values for the parameters, in the above equation, we must determine what range of values that v_a can obtain spirometery. This is done in the next section.

Spirometeric Parameter Ranges

Tables 1 and 2 list the average volume flow rates with the corresponding air velocitics and average lung volumes respectively [9],[10],[11]. The following definitions will clarify the terms used in the tables.

Maximum expiratory/inspiratory volume flow rate (MEV/MJV) - the maximum volume flow rate obtained after maximum inspiration/expiration.

Maximum breathing capacity (MBC) - the maximum sustained volume flow rate under physical stress.

Spontaneous breathing capacity (SBC) - the volume flow rate under quiet rest conditions.

Total lung capacity (TLC) - the total volume of lungs upon maximum inhalation.

Vital capacity (VC) - the largest volume of air that can be expired after a maximum inspiration.

Inspiratory reserve volume (IRV) - the volume capable of being inspired after quiet expiration.

Expiratory reserve volume (ERV) - the volume capable of being expired after quiet inspiration.

The air velocities given in table 1 were determined by the following equation

$$v_a = \frac{\text{volume flow rate}}{\text{cross sectional area}} = \frac{4\dot{v}}{\pi d_o^2} \qquad (21)$$

where $\dot{v}$ is the volume flow rate and d_o is the diameter of the circular breathing tube. These air velocities were obtained if breathing is done through a 1.5 inch diameter tubing, which is assumed not to affect the normal breath rates.

The lung volumes are determined by the system by integrating the air velocity over the cross sectional area used in equation 21. Table 2 is included to give the range of volumes that will be encountered.

Table 1. - Spirometer Volume Flow Rates

type	volume flow rate(liters/sec)	velocity(meters/sec)
MEV	12.0	10.7
MIV	9.0	8.0
MBC	1.67	1.48
SBC	0.17	0.150

Table 2. - Spirometeric Air Velocities

type	volume(liters)
TLC	6.00
VC	5.0
IRV	2.5
ERV	2.0

Table 3. - Stability Requirements

$$T_2 > T_1$$

$$\omega_n/f > 6(T_2^2 - T_1^2)/(T_2^3 - T_1^3)$$

$$\omega_n < \sqrt{(2/3(T_2^2 - T_2^2))}$$

Lock Range Requirements

In this section we will check to see if the lock range of the DPLL is sufficient for our purposes.

Neglecting changes in c and setting $\cos\theta = 1$ equations 6 and 20 become

$$M/8K_2N(1 + \tfrac{1}{2}K_2) > v_a/c'.$$

Using c = 343.57 m/s, $K_2 = 8$ (which is the minimum value of K for a K-counter using the SN74LS297 digital PLL filter), and setting the system clocks equal (i.e. M = 4N), v_a satisfies

$$v_a < 20.21 \text{ m/sec}$$

which is true for the maximum value obtained in spirometery (v_a(MEV)=10.7 m/s).

Transducer-filter Delay Affects

Now we will look more closely at the effect transducer-filter delays (T_k) have on the static response of the system. Starting at equations 1 and 2 we must include the transducer delays T_k as

$$T_1 = d_1/(c + v_a\cos\phi) + T_{k1}$$

and

$$T_2 = d_2/(c + v_a\cos\phi) + T_{k2}.$$

Using the same arguments as before, the phase error is given by

$$\phi_{e1} = K_{d3}\omega\{(d_2 - d_1)/(c + v_a\cos\theta) + (T_{k2} - T_{k1})\}. \qquad (22)$$

Substituting $T_e = T_{k2} - T_{k1}$, and following the same steps which led to equations 6 and 7 of chapter 2, we obtain for perfect phase-lock (derivation given in Appendix A)

$$(\omega_o - \omega_c)/\omega_c = (c/c' + v_a\cos\theta/c' - 1)\cdot(1-(c + v_a\cos\theta)(T_e)/(d_2 - d_2))^{-1}. \qquad (23)$$

By comparing this with equation 6 and knowing $10v_a < c$, it is seen that the conditions for ideal response is

$$|(c\,T_e)/(d_2 - d_1)| \ll 1. \qquad (24)$$

Thus is necessary to maximize the separation of the receivers for any given transducer-filter delay. For c = 343.57 m/s (20 C 0.0% humidity) (d_2-d_1)=0.01 m and T_e = 2.5 microseconds the resulting error from the ideal of equation 21 is less than 1%.

Each T_k is composed of two parts; the receiver delay and the transmitter delay. For each half of the system, as shown in figure 1, the same transmitter is used for each path. Therefore, T_e is composed of only the difference between receiver delays. Because of the fine tolerences required in manufacturing piezoceramic air transducers closely matched transducers are not uncommon and any slight difference can be tuned to a very small difference, using common crystal tuning techniques.

CHAPTER 5

DYNAMIC RESPONSE

In this chapter we will study the stability requirements, how the system obtains perfect phase-lock, and the maximum allowable step change in air velocity.

Stability Requirements

Figure 6 shows one-half the system in signal flow graph representation. Using Masons Loop Rule [12], we obtain the transfer function

$$\phi_{e_1}/f_c = sK_{d_3}P(s) \div (s^2 + 2\zeta\omega_n s + \omega_n^2) - K_{d_3}(2\zeta\omega_n s + \omega_n^2)P(s) \qquad (25)$$

where

$$P(s) = \exp(-sT_1) \cdot (1 - sT_1) - \exp(-sT_2) \cdot (1 - sT_2),$$

$$\zeta = \tfrac{1}{2}(\omega_1/\omega_2)^{\frac{1}{2}},$$

$$\omega_n = (\omega_1 \cdot \omega_2)^{\frac{1}{2}},$$

$$\omega_1 = (K_{d_1}Mf_c(/(2K_1N),$$

and

$$\omega_2 = (K_{d_2}Mf_c)/(4K_2NL).$$

First, we will look at the stability requirements. The Routh-Hurwitz Stability Criterion [13] can be applied to this system only if the delay terms are approximated by a few terms of the power series

$$\exp(-sT) = 1 - sT + (sT)^2/2! - (sT)^3/3! + \ldots.$$

We will use the first three terms of the series. Therefore, the Routh-Hurwitz criterion will yield only approximate stability information. Substituting into P(s) we obtain

$$P(s) \doteq \tfrac{1}{2}\{4s(T_2 - T_1) - 3s^2(T_2^2 - T_1^2) + s^3(T_2^3 - T_1^3)\}. \quad (26)$$

At this point we come to the first major problem. Substituting equation 26 into 25, we find that the system, as it is configured, will always be unstable. This arises because of the minus sign in the denominator of equation 25. This problem is easily corrected, and in doing so we reduce the number of parts used in the system. What is done is shown in figure 7. We eliminate the third phase detector and place the second acoustic path inside the phase-lock loop feedback path. The following transfer function results from these changes

$$\phi_{e1}/f_c = -sP(s)/(s^2 + (2\zeta\omega_n s + \omega_n^2)P(s)) \quad (27)$$

The derivation of equation 27 is given in Appendix B.

Notice that this modification has two effects; the minus sign is eliminated, and the order of the transfer function is reduced. Substituting equation 26 into 27 we obtain

$$\phi_{e1}/f_c = -s((T_2^3 - T_1^3)s^2 - 3(T_2^2 - T_1^2)s + 4(T_2 - T_1)) \div \quad (28)$$
$$(A_3 s^3 + A_2 s^2 + A_1 s + A_0)$$

where

$$A_3 = 2\,\zeta\omega_n(T_2^3 - T_1^3),$$

$$A_2 = \omega_n^2(T_2^3 - T_1^3) - 6\zeta\omega_n(T_2^2 - T_1^1),$$

$$A_1 = 2 + 8\zeta\omega_n(T_2 - T_1) - 3\omega_n^2(T_2^2 - T_1^2),$$

and

$$A_o = 4\omega_n^2(T_2 - T_1).$$

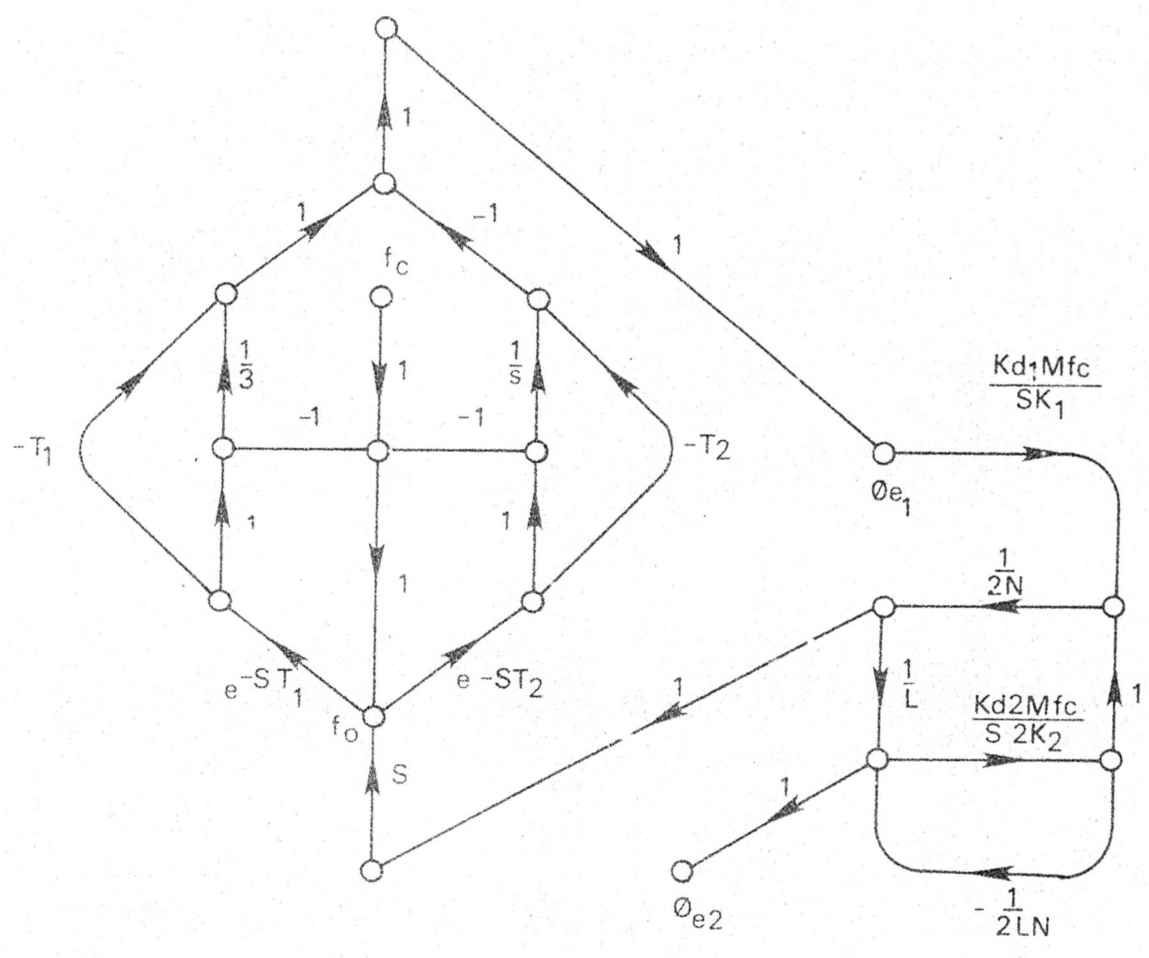

Figure 7. One-half of modified system in signal flow graph representation.

The Routh-Hurwitz stability requirements are

$$A_i > 0 \quad i = 0 \text{ to } 3,$$

and

$$A_2 A_1 - A_3 A_0 > 0.$$

The first four requirements are fulfilled if

$$T_2 > T_1$$

$$\omega_n/\zeta > 6(T_2^2 - T_1^2)/(T_2^3 - T_1^3)$$

$$\omega_n < \{2/(3(T_2^3 - T_1^3))\}^{1/2}.$$

Whether all five requirements can be fulfilled is dependent on the values of T_1 and T_2. These requirements are listed in Table 3.

It is important to recognize that the steady-state response of the modified system does not differ from the response of the original system.

Appendix C contains plots of s-plane root locations of the modified system under varying conditions. As can be seen from these plots, the system can usually be stabilized for typical system values and the stability range is highly dependant upon transducer delay and acoustic path distances. Two major points can be drawn from these s-plane plots. First, decreasing the transducer delays or decreasing acoustic path distances has a marked improvement on the system response at the cost of having to raise the DPLL resonance frequency which is determined primarily by the clock frequency of the DPLL-filter integrated circuit. Another method of raising the resonance frequency is to use different clock frequencies for the various DPLL components (i.e. M≠4N). Both of these methods would reduce the resolution of the output (refer to equations 25 and 18).

Second, reducing the separation distance between the two receivers also improves the system response.

Appendix D contains the Fortran program and parameter values used to generate the data points of the s-plane plots.

Step Input Response

The system response to a step change in air velocity is controlled by a highly non-linear equation and evades simple analysis. The transfer function given by equation 28 does not give the response required but is only used to determine the systems stability. What we would be looking for is the output's (ϕ_{e2}) response to changes in air velocity. The steady-state response shows that this output is 100% sensitive to changes in air velocity but tells us nothing on how this steady-state value is reached.

Maximum Allowable Step Input

The next question we must answer is what is the maximum step change in air velocity v_a that is allowed before an ambiguity occurs in the phase difference. This occurs when $|\phi_{e1}| > \pi$. Starting with c = c' neglecting cosθ and changes in ω_o (i.e. $\omega_o = \omega_c$) we obtain

$$\pi < |\omega_c(d_2 - d_1)/c' - \omega_o(d_2 - d_1)/c + v_a \cos\theta| \approx$$

$$|-v_a \, \omega_c(d_2 - d_1)/(c')^2|.$$

For $c'=343.0$ m/s, $\omega_c = 2\pi \cdot 40K$ rad/s, and $d_2 - d_1 = 0.01$ m,

$$v_a > \pi(c')^2/(\omega_c(d_2 - d_1)) \approx 147.0 \text{ m/s}.$$

This is enourmous, and for smaller separation becomes even greater. Therefore, this constraint presents no problems for most applications. This ambiguity occurs because of the saw-tooth shape of the phase detector transfer function.

CHAPTER 6

SUMMARY

In this thesis, we have been concerned with quantitative mathematical modeling of the various components of the system. The differential equations describing the dynamic and static performance of the system was utilized to construct this mathematical mod

Various design considerations are given in the text to aid in construction of the system with the desired characteristics. Major advantages resulting from the designs used include:

1) Only the air temperature at the time of system calibration need be known to completely determine air velocities and temperatures measured.

2) The cost of construction, as compared to other similar devi ... is significantly reduced by configuring the system so that inexpensive piezoelectric transducers can be used.

3) Long term reliability and durability results from the use of solid state electronic components and the absence of mechanical parts with the exception of the piezoelectric transducers.

Further considerations would be to determine energy balances by either estimating or measuring mass flow rates and appling the laws of thermodynamics thus enabling the user to determine breathing efficiencies.

APPENDICIES

APPENDIX A

DERIVATION OF RELATIVE FREQUENCY SHIFTS

The phase error under zero air velocity conditions is

$$\phi_e = \omega_c((d_2 - d_1)/c' + T_e \tag{1}$$

and the phase error under non-zero air velocity conditions is

$$\phi_e = \omega_o((d_2 - d_1)/(c + v_a\cos\ ) + T_e). \tag{2}$$

Under perfect phase-lock conditions these two are equal, and can be equated. Doing this we get

$$\omega_c((d_2 - d_1)/c' + T_e) = \omega_o((d_2 - d_1)/(c + v_a\cos\ )+T_e). \tag{3}$$

Rearranging (3) in the following steps;

$$\omega_c(d_2 - d_1)/c' - \omega_o(d_2 - d_1)/(c + v_a\cos\phi) = T_e(\omega_o - \omega_c),$$

$$c + v_a\cos\phi - \omega_o c'/\omega_c = c' \cdot T_e(\omega_o - \omega_c)/((d_2 - d_1)\omega_c),$$

$$\omega_o/\omega_c = (c + v_a\cos\phi)/c' + T_e(c + v_a\cos\phi)(\omega_c - \omega_o)/((d_2 - d_1)\omega_c),$$

$$(\omega_o - \omega_c)/\omega_c = c/c' + v_a\cos\phi/c' - 1 + T_e(c + v_a\cos\phi)(\omega_c-\omega_o)/((d_2-d_1)\omega_c),$$

$$((\omega_o - \omega_c)/\ _c)(1 - (c + v_a\cos\phi)(T_e)/(d_2-d_1)) = c/c' + v_a\cos\phi/c' - 1,$$

and finally,

$$(\omega_o-\omega_c)/\omega_c = (c/c' + v_a\cos\phi/c' - 1)\cdot(1 - (c + v_a\cos\phi)(T_e)/(d_2-d_1))^{-1}.$$

APPENDIX B

DERIVATION OF MODIFIED SYSTEM TRANSFER FUNCTION

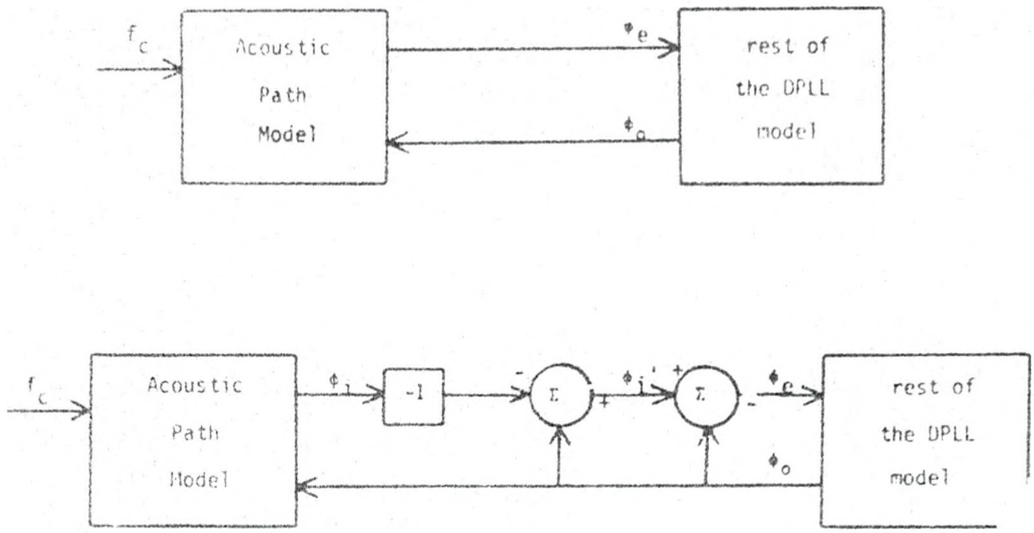

Figure 8. Modified System Block Diagram.

Careful inspection of the two systems in figure 8 show that they are identical. The DPLL Transfer function is

$\phi_o/\phi_i' = N(s)/D(s) = (2\zeta\omega_n s + \omega_n^2)/(s^2 + 2\zeta\omega_n s + \omega_n^2)$. (1)

Also, ϕ_e is defined as

$\phi_e/\phi_i' = s^2/D(s)$. (2)

From figure 8 we obtain; $\phi_i' = -\phi_i + \phi_o$, (3)

and from the text the acoustic path function is

$\phi_i = P(s)\phi_o + P(s)f_c/s$. (4)

Combining (1) and (3); $\phi_i = \phi_o(1 - D(s)/N(s))$, (5)

(1) and (2) $\phi_o = \phi_e N(s)/s^2$, (6)

and (4) and (5) $P(s)f_c/s = \phi_o(1 - D(s)/N(s) - P(s))$. (7)

Finally, combining (1), (6), and (7) we obtain

$\phi_e/f_c = - sP(s)/(s^2 + P(s)N(s))$.

APPENDIX C

S-PLANE ROOT LOCUS PLOTS

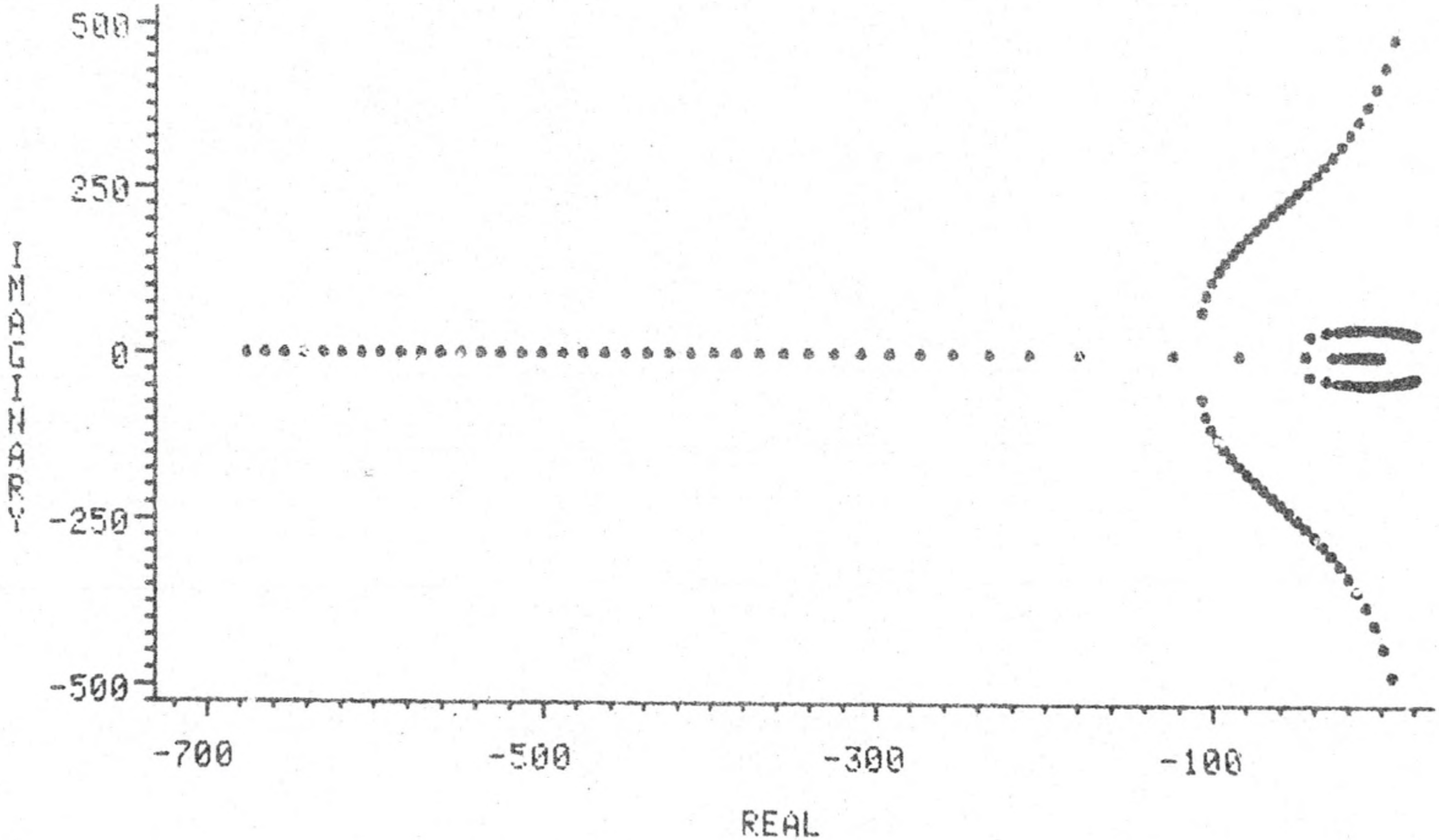

Figure 9. S-plane Root locus Plot.

ζ = .707, ω_n = 76 to 1000., T_k = 30.ms, $d_2 - d_1$ = 1.0 cm.

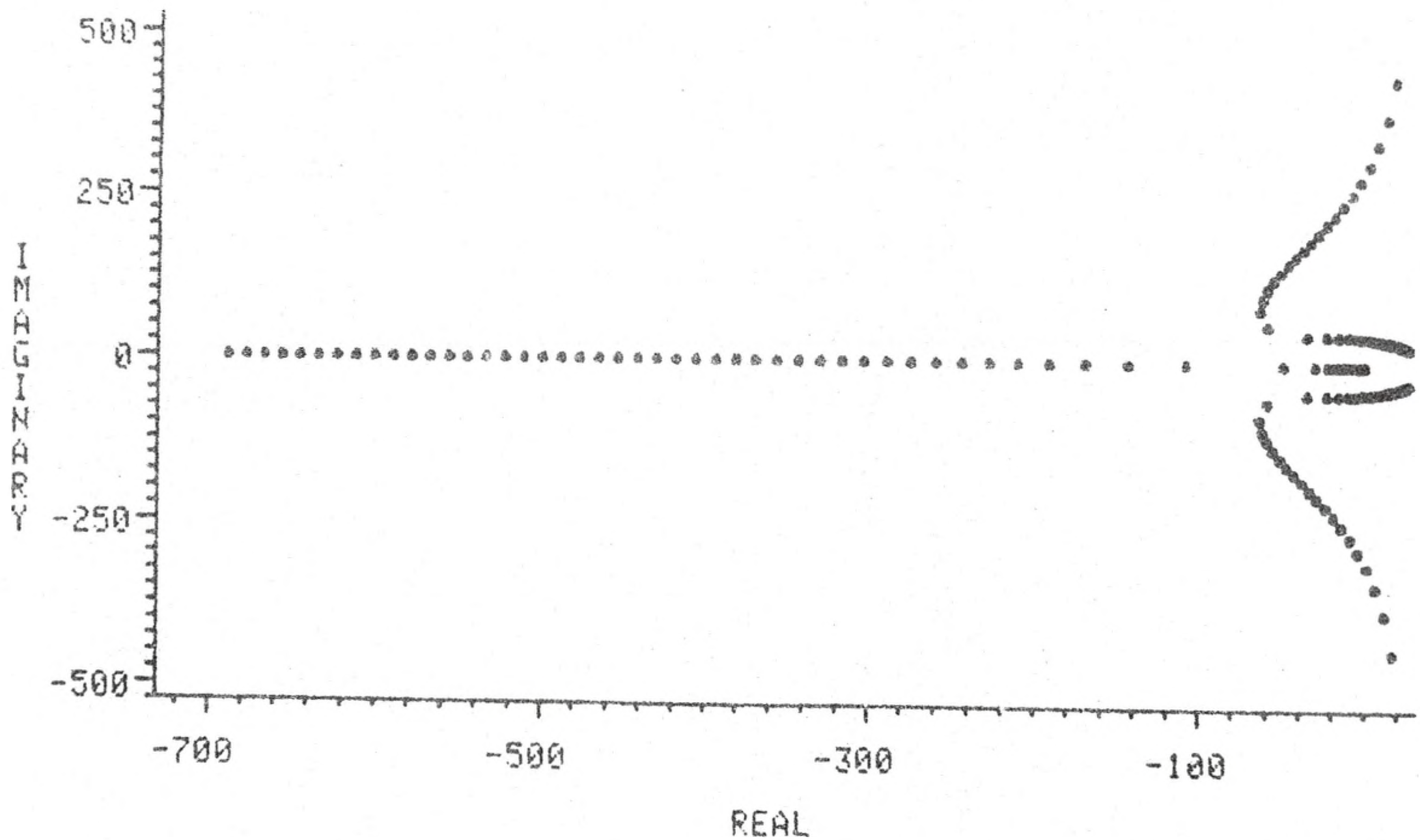

Figure 10. S-plane Root locus Plot.

ζ = .707, ω_n = 46 to 1000., T_k = 30.ms, $d_2 - d_1$ = 2.0 cm.

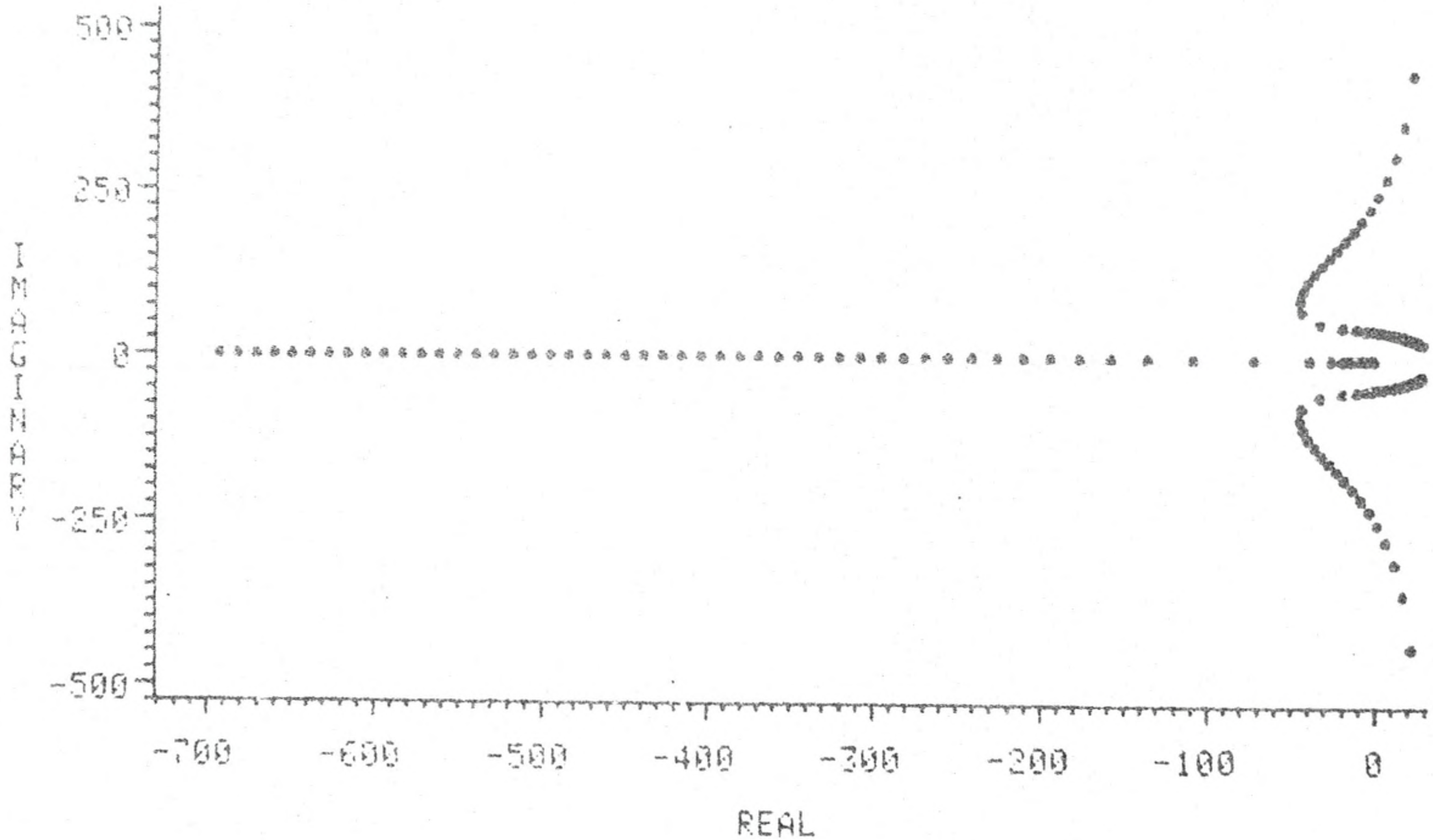

Figure 11. S-plane Root locus Plot.

ζ = .707, ω_n = 31 to 1000., T_k = 30.ms, d_2-d_1 = 3.0 cm.

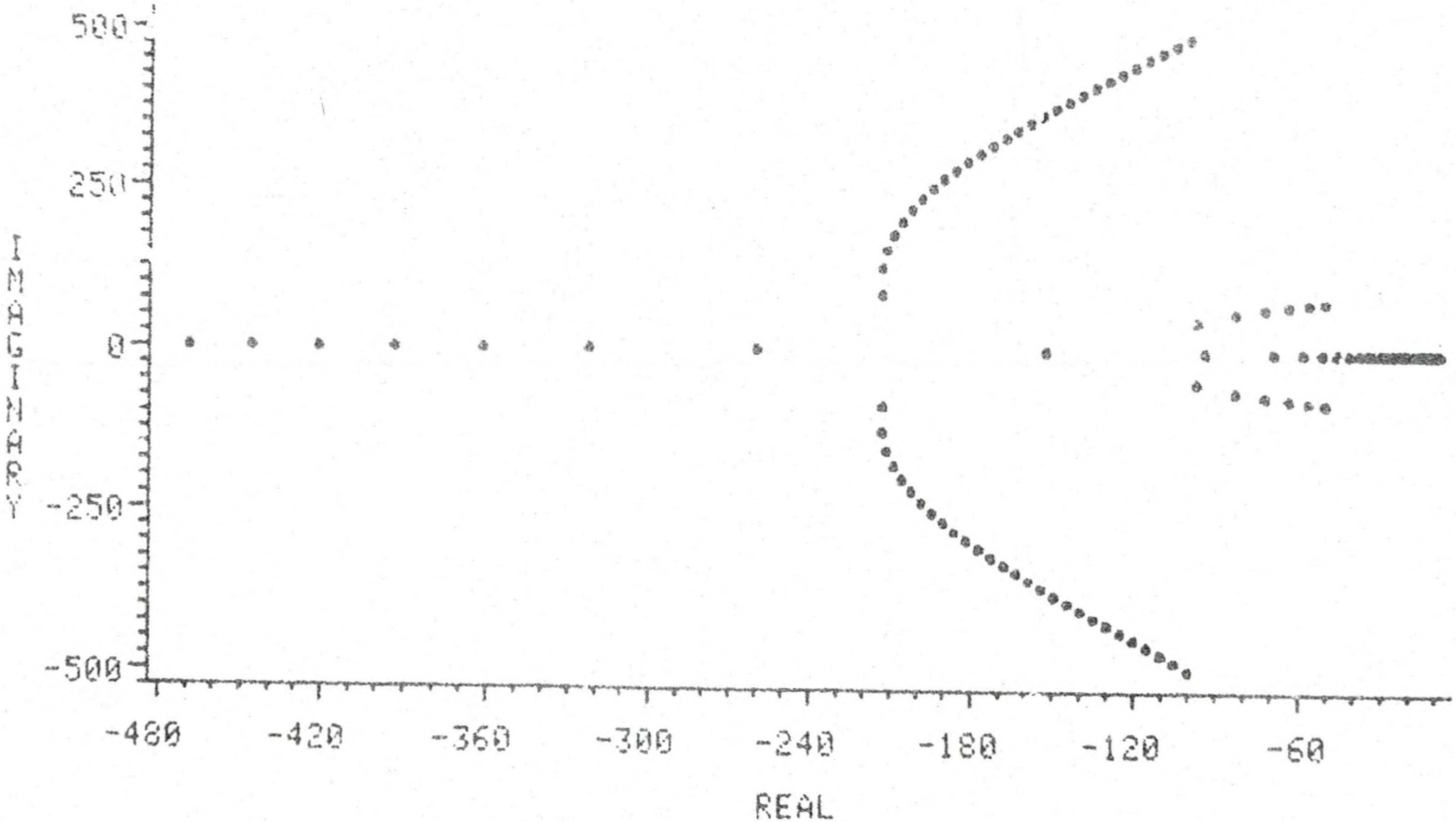

Figure 12. S-plane Root locus Plot.

ζ = .707, ω_n = 480 to 1000., T_k = 15.ms, $d_2 - d_1$ = 0.5 cm.

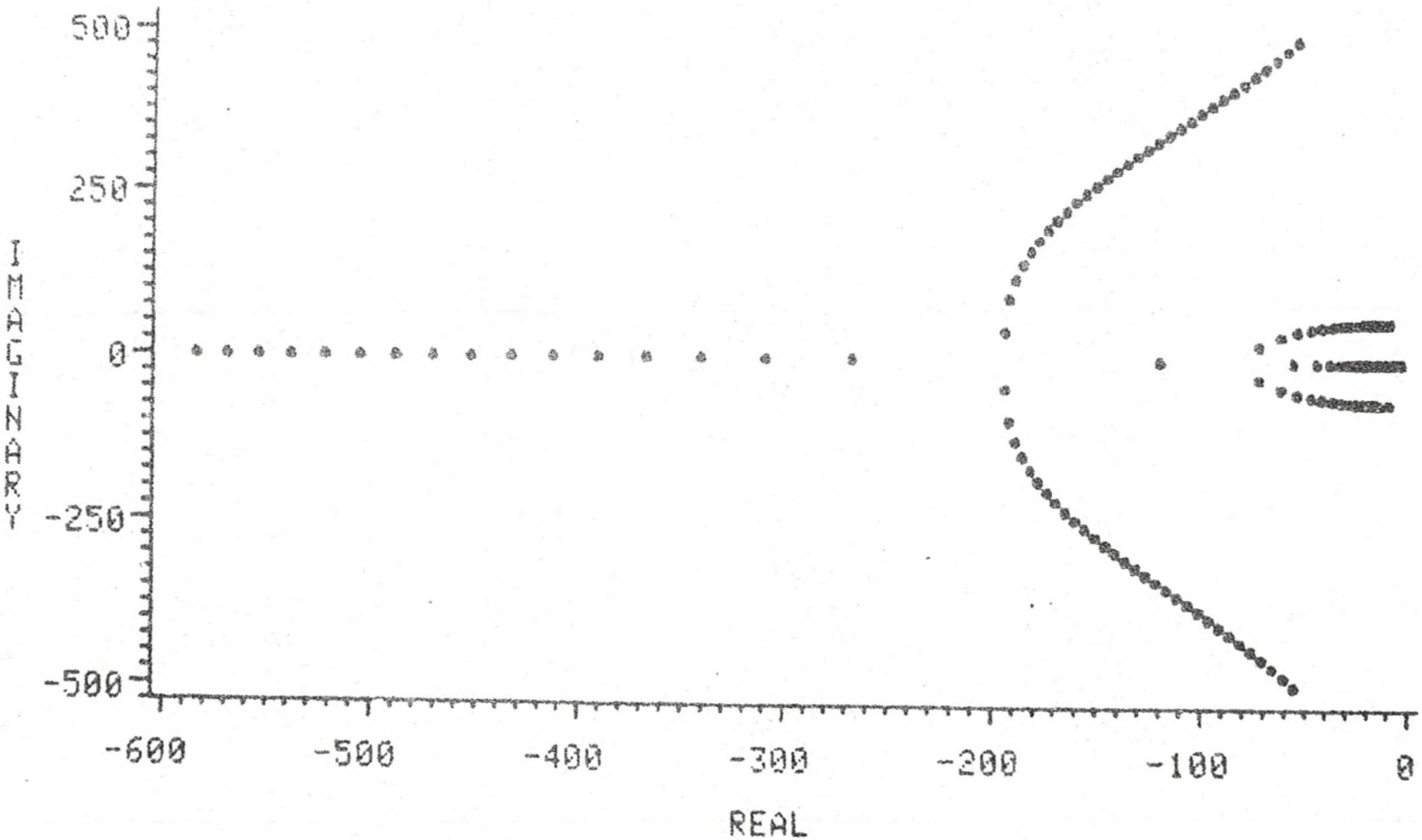

Figure 13. S-plane Root locus Plot.

ζ = .707, ω_n = 300 to 1000., T_k = 20.ms, $d_2 - d_1$ = 0.5 cm.

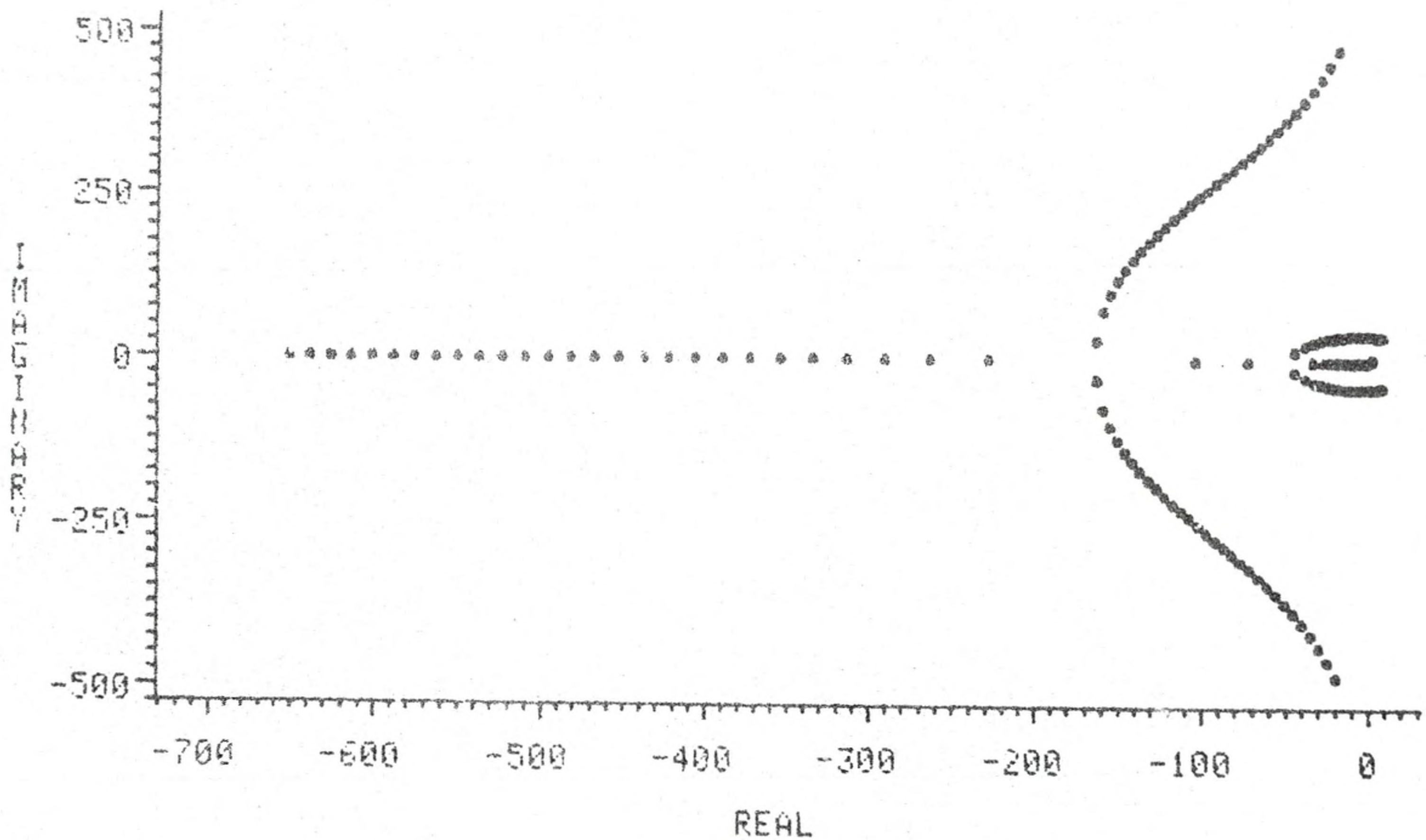

Figure 14. S-plane Root locus Plot.

ζ = .707, ω_n = 150 to 1000., T_k = 30.ms, d_2-d_1 = 0.5 cm.

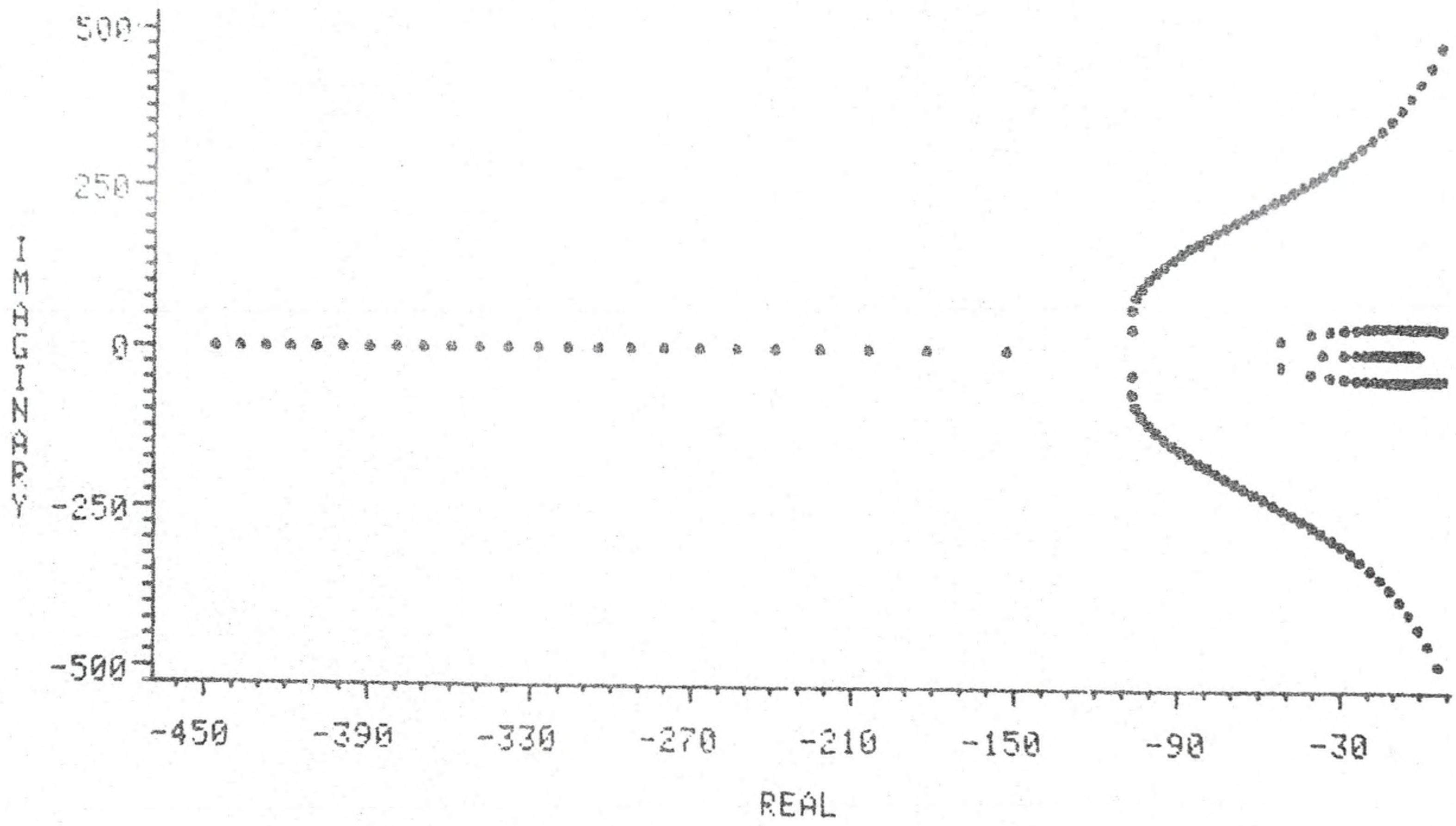

Figure 15. S-plane Root locus Plot.

$\zeta = 1.00$, $\omega_n = 100$ to 1000., $T_k = 30.$ms, $d_2 - d_1 = 0.5$ cm.

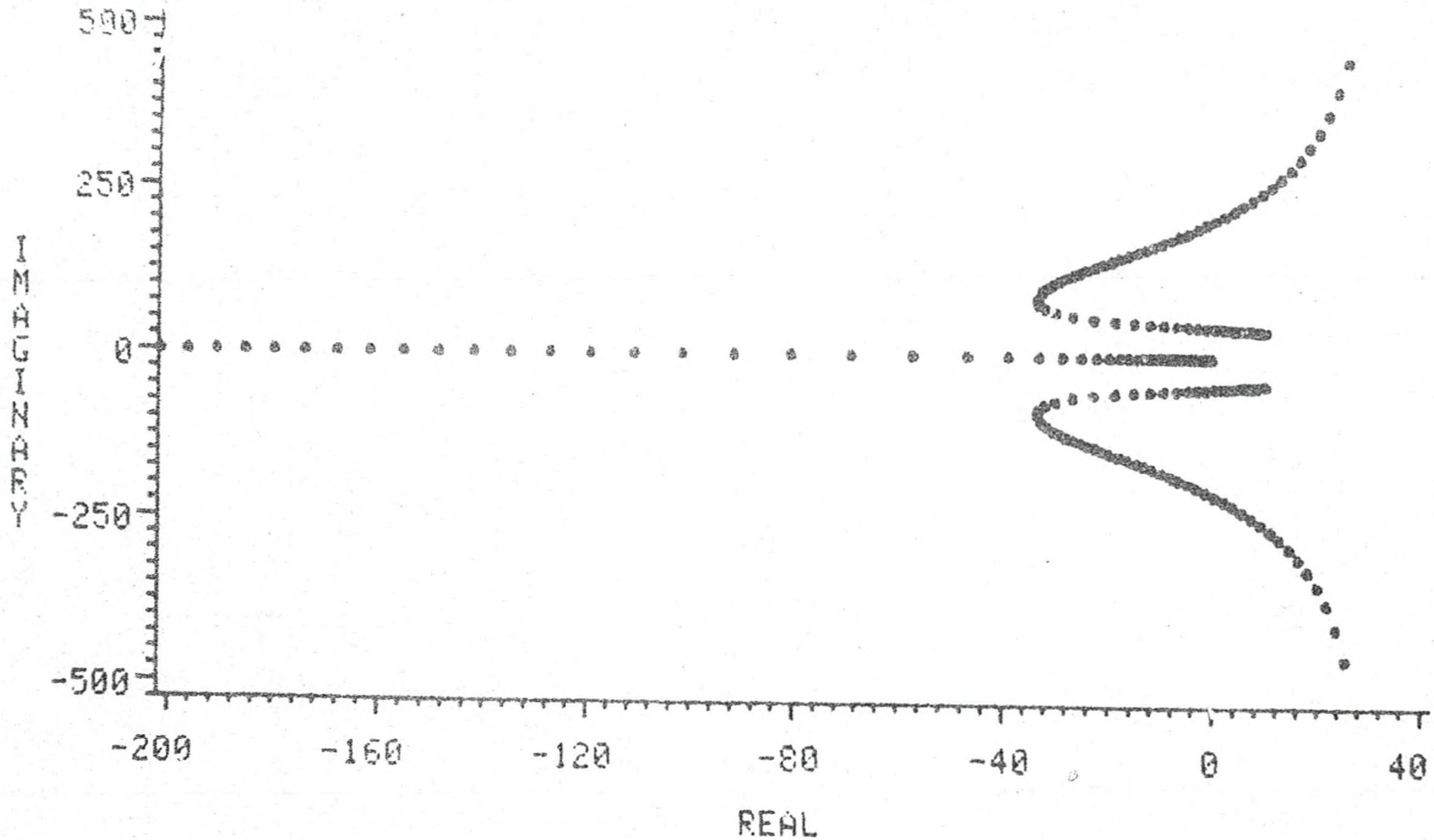

Figure 16. S-plane Root locus Plot.

$\zeta = 2.0$, ω_n = 60 to 1000., T_k = 30.ms, $d_2 - d_1$ = 0.5 cm.

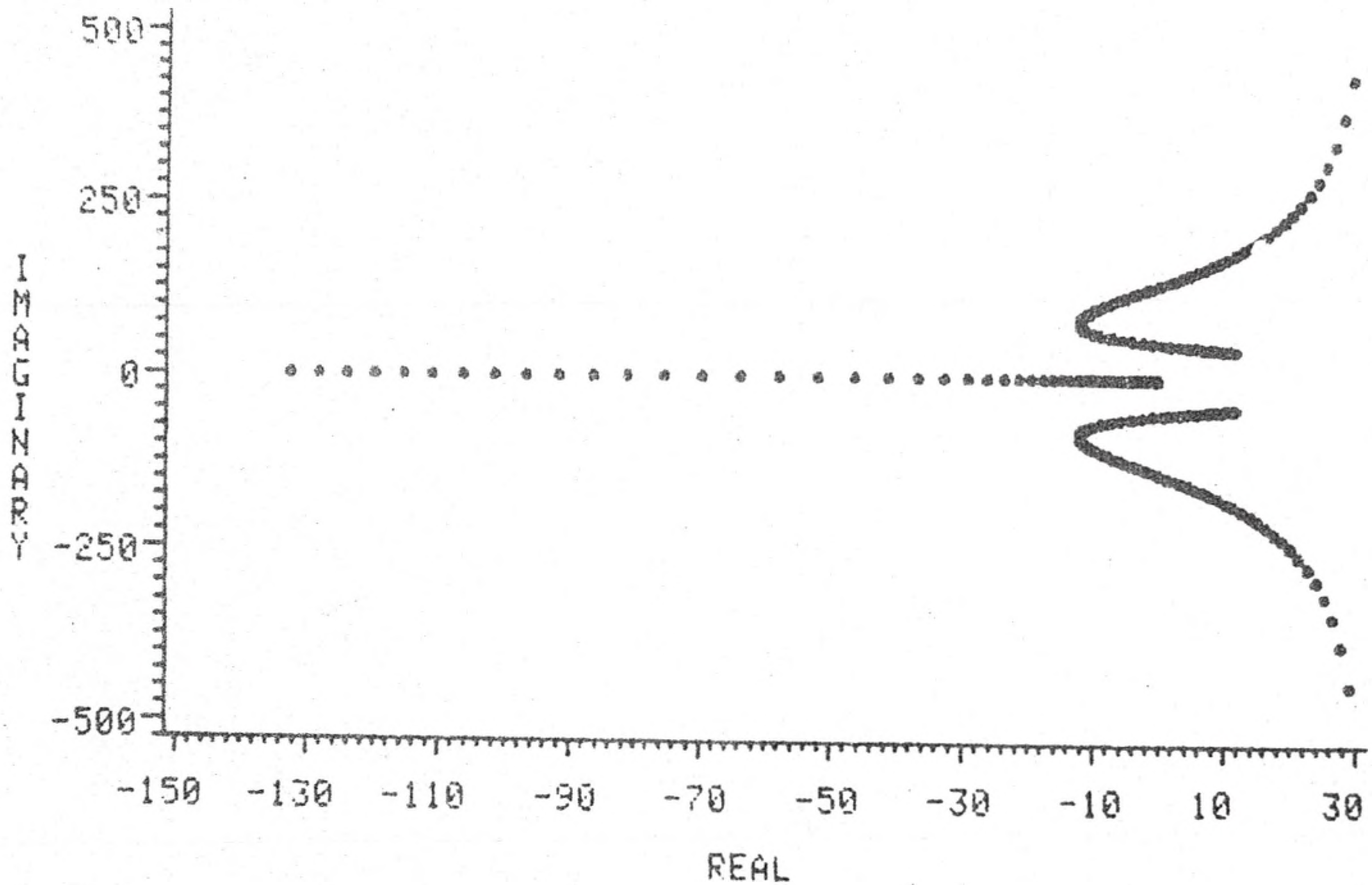

Figure 17. S-plane Root locus Plot.

$\zeta = 2.83$, $\omega_n = 46$ to 1000., $T_k = 30.$ms, $d_2 - d_1 = 0.5$ cm.

APPENDIX D

FORTRAN PROGRAM LISTING

```
      DIMENSION DELAY1(30),DELAY2(30),P1(30),P2(30
),POLES(30)
      DIMENSION PR(30),PI(30),D(22),ZEROS(30),ZR(3
0),ZI(30)
      DIMENSION A(30),B(30),C(30),PLLNUM(30),P(30)
,E(25)
C ******************************************
****
C
C        THIS SECTION GENERATES THE POLYNOMIAL P(S
).
C        (SEE TEXT OF THESIS.)
C
C           P(S) = COEFFICIENT POLYNOMIAL OF P
C             IP = ORDER OF P
C
      DO 100 III = 3,16
      D1 = .05
      D2 = .055
      C0 = 343.0
      VA = 0.0
      ID = 2
      TFIL = 30.E-3
      T1 = D1 / (VA + C0) + TFIL
      T2 = D2 / (VA + C0) + TFIL
      CALL PDELT(T1,ID,DELAY1)
      CALL PDELT(T2,ID,DELAY2)
      P1(1) = 1.0
      P1(2) = -T1
      IP1 = 1
      P2(1) = 1.0
      P2(2) = -T2
      IP2 = 1
      G = -1.
      CALL PMUL(B,IB,DELAY1,ID,P1,IP1)
      CALL PMUL(A,IA,DELAY2,ID,P2,IP2)
      CALL FORM(G,A,IA,B,IB,P,IP)
C *******************************************
**********
C
C         THIS SECTION GENERATES THE THE PHASE-LO
CK LOOP
C         TRANSFER FUNCTION POLYNOMIALS.
C
C           OMEGA1 = RESONANCE FREQUENCY OF FIRST
 LOOP
C           OMEGA2 = RESONANCE FREQUENCY OF SECON
D LOOP
C           OMEGAN = NATURAL RESONANCE FREQ. OF T
OTAL LOOP
```

```
C          FREQC = FREE RUNNING FREQ. OF PHASE-LOCKED LOOP
C           DAMP = DAMPING FACTOR OF PHASE-LOCKED LOOP
C
C      PLLNUM(S) = NUMERATOR POLYNOMIAL OF PLL.
C          IPLLN = ORDER OF NUMERATOR
C
      L = 1.0
      N = 256 / (2*L)
      M = 4*N
      FREQC = 40000.
      K1 = 2**(III)
      K2 = K1
      KD1 = 2
      KD2 = 2
      OMEGA1 = (KD1 * M * FREQC) / (2 * K1 * N)
      OMEGA2 = (KD2 * M * FREQC) / (4 * K2 * L * N)
      OMEGAN = SQRT(OMEGA1*OMEGA2)
      DAMP = SQRT(OMEGA1/OMEGA2) / 2.0
      PLLNUM(1) = OMEGAN**2
      PLLNUM(2) = 2*DAMP*OMEGAN
      IPLLN = 1
C ***************************************************************
C
C     THIS SECTION FORMS THE CHARACTERISTIC EQUATION
C     OF ONE-HALF OF THE SYSTEM.
C     IT THEN FINDS THE LOCATION OF THE POLES OF THE
C     SYSTEM IN THE S-PLANE.
C
C          T(S) = CHARACTERISTIC EQUATION
C            IT = ORDER OF T(S)
C          U(S) = REAL ROOT ARRAY
C          V(S) = IMAGINARY ROOT ARRAY
C
      G = 1.0
      D(1) = 0.0
      D(2) = 0.0
      D(3) = 1.0
      IDD = 2
      CALL PMUL(C,IC,PLLNUM,IPLLN,P,IP)
      CALL FORM(G,C,IC,D,IDD,POLES,IPOLES)
      CALL PROOT(IPOLES,POLES,PR,PI,1)
      PRINT 1, OMEGAN,DAMP
    1 FORMAT(1X,'OMEGAN=',F15.5 ,2X,'DAMPING FACTOR=',F15.5)
```

```
           PRINT 2
         2 FORMAT(1X,'      ')
           PRINT 3
         3 FORMAT(1X,'POLES:          SIGMA               J
-W')
           PRINT 4, (PR(I),PI(I), I = 1 , IPOLES)
         4 FORMAT(10X,F15.5,2X,F15.5)
           E(1) = 0.0
           E(2) = -1.0
           IE = 1
           CALL PMUL(ZEROS,IZEROS,E,IE,P,IP)
           CALL PROOT(IZEROS,ZEROS,ZR,ZI,1)
           PRINT 2
           IF (IPOLES.GT.IZEROS) J = IPOLES
           IF (IZEROS.GE.IPOLES) J = IZEROS
           DO 100 I = 1, J
           IF (PR(I)+PI(I)+ZR(I)+ZI(I).EQ.0.0) GO TO 10
0
           WRITE(8,*) PR(I),PI(I),ZR(I),ZI(I)
       100 CONTINUE
           PRINT 5
         5 FORMAT(1X,'ZEROS:          SIGMA               J-
W')
           PRINT 4, (ZR(I),ZI(I), I = 1 , IZEROS)
           STOP
           END
      C *************************************************
******
           SUBROUTINE NORMP(X,IX,EPS)
      C    THIS SUBROUTINE ZEROS COEFFICIENTS OF A POLYNO
MIAL
      C    THAT ARE LESS THAT A THRESHOLD VALUE, THUS RED
UCINGG
      C    THE ORDER OF THE POLYNOMIAL.
      C
      C          X = COEFFICIENT ARRAY, CONSTANT FIRST
      C         IX = ORDER OF POLYNOMIAL + 1
      C        EPS = THRESHOLD OF THE SEARCH
           DIMENSION X(10)
         1 IF (IX) 4,4,2
         2 IF (ABS(X(IX)) - EPS) 3,3,4
         3 IX = IX - 1
           GO TO 1
         4 RETURN
           END
      C ***********************************************
**********
           SUBROUTINE PDELT(T,N,DELAY)
      C    THIS SUBROUTINE GENERATES THE NTH ORDER POLY
NOMIAL
```

```
C      APPROXIMATION TO A DELAY (I.E. EXP(-TS)).
C
C       DELAY = POLYNOMIAL APPROXIMATION OF DELAY
C           N = ORDER OF POLYNOMIAL N[= 10
C           T = DELAY TIME
C
       DIMENSION DELAY(11)
       FACT = 1.
       SIGN = 1.0
       MINUS = -1.0
       DO 10 I = 1,N
       SIGN = SIGN * MINUS
       FACT = FACT * I
    10 DELAY(I+1) = SIGN * (T**I) / FACT
       DELAY(1) = 1.
       RETURN
       END
C ********************************************************
       SUBROUTINE FORM(G,A,N,B,M,C,IX)
C  THIS SUBROUTINE FORMS THE WEIGHTED SUM OF TWO POLYNOMIALS
C
C           C(S) = B(S) + G * A(S)
C
C           G = SCALER WEIGHTING FACTOR
C           A = POLYNOMIAL COEFFICIENT ARRAY FOR A(S),CONSTANT FIRST
C           N = ORDER OF A(S), N[= 10
C           B = POLYNOMIAL COEFFICIENT ARRAY FOR B(S),CONSTANT FIRST
C           M = ORDER OF B(S), M[= 10
C           C = POLYNOMIAL COEFFICIENT ARRAY FOR RESULTING C(S)
C          IX = ORDER OF C(S)
C
       DIMENSION A(11),B(11),C(11)
       IF(N-M) 1,2,2
     1 IX=M+1
       GO TO 3
     2 IX=N+1
     3 DO 4 I=1,IX
     4 C(I)=B(I)+G*A(I)
       IX=IX-1
        RETURN
       END
C ******************************************************
       SUBROUTINE PEXCG(A,IA,B,IB)
```

```
C  THIS SUBROUTINE REPLACES A WITH B (A IS DESTROY
ED)
C
C                A(S) = B(S)
C
C                A = ARRAY OF A(S)
C               IA = ORDER OF A
C                B = ARRAY OF B(S)
C               IB = ORDER OF B
C
        DIMENSION A(1),B(1)
        JJ=IB+1
        DO 1 I=1,JJ
      1  A(I)= B(I)
        IA=IB
        RETURN
        END
C ***********************************************
*******
        SUBROUTINE PMUL(Z,IZ,X,IXA,Y,IYA)
C  THIS SUBROUTINE FORMS PRODUCT OF TWO POLYNOMIAL
S
C
C              Z(S) = X(S) * Y(S)
C
C                Z = RESULTING COIEFFICIENT ARRAY, CO
NSTANT FIRST
C               IZ = ORDER OF Z, [=8
C                X = COEFFICIENT ARRAY OF X(S), CONST
ANT FIRST
C              IXA = ORDER OF X
C                Y = COEFFICIENT ARRAY OF Y(S), CONST
ANT FIRST
C              IYA = ORDER OF Y
C
        DIMENSION X(10),Y(10),Z(10)
        IX=IXA+1
        IY=IYA+1
        IF (IX*IY) 10,10,20
     10 IZ = 0
        GO TO 50
     20 IZ = IX + IY
        DO 30 I = 1, IZ
     30 Z(I) = 0.0
        DO 40 I = 1, IX
        DO 40 J = 1, IY
        K = I + J - 1
        Z(K) = X(I) * Y(J) + Z(K)
     40 CONTINUE
        IZ = IZ - 2
```

```
   50 RETURN
      END
C *************************************************************
      SUBROUTINE PROOT(N,A,U,V,IR)
C  THIS SUBROUTINE USES A MODIFIED BARSTOW METHOD TO FIND
C  THE ROOTS OF A POLYNOMIAL.
C
C          N = DEGREE OF POLYNOMIAL, N[=19
C          A = POLYNOMIAL COEFFICIENT ARRAY.
C          U = REAL ROOT ARRAY
C          V = IMAGINARY ROOT ARRAY
C         IR = +1 IF POLYNOMIAL WRITTEN AS: A(1)+A(2)S+A(3)S**2+...
C            = -1 IF POLYNOMIAL WRITTEN AS; A(1)S**N+A(2)S**(N-1)+..
C
      DIMENSION A(20),U(20),V(20),H(21),B(21),C(21)
      IREV = IR
      NC = N + 1
      DO 1 I = 1, NC
    1 H(I) = A(I)
      P = 0.
      Q = 0.
      R = 0.
    3 IF (H(1)) 4,2,4
    2 NC = NC - 1
      V(NC) = 0.
      U(NC) = 0.
      DO 1002 I = 1, NC
 1002 H(I) = H(I+1)
      GO TO 3
    4 IF (NC - 1) 5,100,5
    5 IF (NC - 2) 7,6,7
    6 R = -H(1)/H(2)
      GO TO 50
    7 IF (NC -3) 9,8,9
    8 P = H(2) / H(3)
      Q = H(1) / H(3)
      GO TO 70
    9 IF (ABS (H(NC-1)/H(NC))-ABS (H(2)/H(1))) 10,19,19
   10 IREV = -IREV
      M = NC / 2
      DO 11 I = 1, M
      NL = NC + 1 - I
      F = H(NL)
      H(NL) = H(I)
```

```
   11 H(I) = F
      IF (Q) 13,12,13
   12 P = 0.
      GO TO 15
   13 P = P/Q
      Q = 1. / Q
   15 IF (R) 16,19,16
   16 R = 1. / R
   19 E = 5.E-10
      B(NC) = H(NC)
      C(NC) = H(NC)
      B(NC+1) = 0.
      C(NC+1) = 0.
      NP = NC - 1
   20 DO 49 J = 1, 1000
      DO 21 I1 = 1, NP
      I = NC - I1
      B(I) = H(I) + R*B(I+1)
   21 C(I) = B(I) + R*C(I+1)
      IF (ABS (B(1)/H(1)) - E) 50,50,24
   24 IF (C(2)) 23,22,23
   22 R = R + 1
      GO TO 30
   23 R = R - B(1)/C(2)
   30 DO 37 I1 = 1, NP
      I = NC - I1
      B(I) = H(I) - P*B(I+1) - Q*B(I+2)
   37 C(I) = B(I) - P*C(I+1) - Q*C(I+2)
      IF (H(2)) 32,31,32
   31 IF (ABS (B(2)/H(1)) - E) 33,33,34
   32 IF (ABS (B(2)/H(2)) - E) 33,33,34
   33 IF (ABS (B(1)/H(1)) - E) 70,70,34
   34 CBAR = C(2) - B(2)
      D = C(3)**2 - CBAR*C(4)
      IF (D) 36,35,36
   35 P = P - 2
      Q = Q * (Q+1)
      GO TO 49
   36 P = P + ( B(2)*C(3) - B(1)*C(4)) / D
      Q = Q + (-B(2)*CBAR + B(1)*C(3)) / D
   49 CONTINUE
      E = E*10.
      GO TO 20
   50 NC = NC - 1
      V(NC) = 0.
      IF (IREV) 51,52,52
   51 U(NC) = 1. / R
      GO TO 53
   52 U(NC) = R
   53 DO 54 I = 1, NC
```

```
   54 H(I) = B(I+1)
      GO TO 4
   70 NC = NC - 2
      IF (IREV) 71,72,72
   71 QP = 1. / Q
      PP = P / (Q * 2.0)
      GO TO 73
   72 QP = Q
      PP = P / 2.0
   73 F = (PP)**2 - QP
      IF (F) 74,75,75
   74 U(NC+1) = -PP
      U(NC) = - PP
      V(NC+1) = SQRT(-F)
      V(NC) = -V(NC+1)
      GO TO 76
   75 IF (PP) 81,80,81
   80 U(NC+1) = -SQRT(F)
      GO TO 82
   81 U(NC+1) = -(PP / ABS(PP) )*( ABS(PP) + SQRT(
F))
   82 CONTINUE
      V(NC+1) = 0.
      U(NC) = QP / U(NC+1)
      V(NC) = 0.
   76 DO 77 I = 1, NC
   77 H(I) = B(I+2)
      GO TO 4
  100 RETURN
      END
```

APPENDIX E

PLL MODEL PARAMETER DEFINITIONS

Symbol	Definition	Units
K_{d1}	Gain of phase detector number 1.	cycles^{-1}
K_{d2}	Gain of phase detector number 2.	cycles^{-1}
K_{d3}	Gain of phase detector number 3.	cycles^{-1}
Mf	Clock frequency of programmable counters.	Hz
Mf_1/K	Gain of programmable divide-by-K_1 counter.	cycles
Mf_2/K	Gain of programmable divide-by-K_2 counter.	cycles
1/N	Gain of divide-by-N counter.	cycles/cycle
1/L	Gain of divide-by-L counter.	cycles/cycle

REFERENCES

[1] R.C. West, CRC Handbook of Chemistry and Physics. Boca Raton, Florida: CRC Press Inc., 1979, page F-117.

[2] S.F. Larsen, F.W. Weiler and J.A. Businger, A Phase-Locked Loop Continuous Wave Sonic Anemonemeter-Thermometer. Journal of Applied Meteorology, Vol. 18, pages 562-568, April 1979.

[3] Ibid., page 567.

[4] D.G. Trohn, Digital Phase-Locked Loop Design Using SN54/74LS297. A Texas Instruments Application Report. Dallas, Texas: Texas Instruments, 1981, page 14.

[5] G. Daryanani, Principles of Active Network Synthesis and Design. New York: John Wiley and Sons, 1976, page 86.

[6] Fink, Electronic Engineers' Handbook. New York: McGraw-Hill Inc., 1975, pages 25-112.

[7] Ibid., pages 25-114.

[8] D.G. Trohn, page 13.

[9] P. Rossier, A. Buhlmann, K. Wiesinger, Respiration Physiologic Principles and Their Clinical Applications. St. Louis: The C.V. Mosby Company, 1960, page 189.

[10] J.G. Scadding, G. Cumming, Scientific Foundations of Respiratory Medicine. Philadelphia: W.B. Saunders Company, 1981, page 126.

[11] S.W. Jacob, C.A. Francone, W.J. Lossow, Structure and Function in Man. Philadelphia: W.B. Saunders Company, 1978, pages 436-438.

[12] R.C. Dorf, Modern Control Systems. Reading, Massachusetts: Addison-Wesley Publishing Company, 1981, pages 57-58.

[13] Ibid., page 148.